Optical pumping in 3He with a laser

P.J. Nacher, M. Leduc

J. Physique **46** (1985) 2057-2073 DÉCEMBRE **1985,** PAGE 2057

Classification
Physics Abstracts
32.80B

Optical pumping in ^{3}He with a laser

P. J. Nacher and M. Leduc

Laboratoire de Spectroscopie Hertzienne de l'E.N.S., 24, rue Lhomond, 75231 Paris Cedex 05, France

(*Reçu le 4 juin 1985, accepté le 22 août 1985*)

Résumé. — Le pompage optique de l'hélium 3 dans l'état fondamental présente certaines particularités liées au fait que la polarisation nucléaire est d'abord obtenue dans l'état métastable 2 ^{3}S et ensuite transférée à l'état fondamental (pompage optique indirect). Ceci introduit des non-linéarités dans les équations d'évolution des populations. Nous présentons ici un modèle numérique de la cinétique du pompage optique de l'hélium 3, qui permet une étude détaillée de l'influence des caractéristiques de la source de pompage (intensité, fréquence, polarisation). On peut jouer d'une façon commode sur ces paramètres à l'aide d'un laser et nous décrivons des expériences faites sur un gaz d'hélium 3 à température ordinaire et à basse température ; leurs résultats sont comparés aux prédictions numériques.

Abstract. — Optical pumping of ground state ^{3}He has several peculiar features because nuclear polarization is first obtained in the metastable 2 ^{3}S state and then transferred to the ground state (indirect optical pumping); this introduces non-linearities in the equation of evolution of the populations. Here we present a numerical calculation of the kinetics of optical pumping in ^{3}He, which allows a detailed study of the influence of the characteristics of the pumping source (intensity, frequency, polarization). These characteristics can be conveniently varied with a laser, and we describe experiments with a ^{3}He gas at room or low temperatures, and compare the results obtained to the numerical predictions.

Introduction.

Optical pumping is an efficient method to create nuclear orientation in gaseous ^{3}He which is far beyond the equilibrium polarization that can be reached at the lowest temperatures and in the highest magnetic fields available at the moment. The method, developed by Colegrove, Schearer and Walters [1], is an extension of ordinary optical pumping [2, 3] where the atomic orientation is directly created in the ground state. In ^{3}He, the nuclear polarization is first obtained by optical pumping in the excited metastable 2 $^3S_1$ state and then transferred to the ground state by metastability exchange collisions. There is a rather large domain of possible applications of optical nuclear polarization of gaseous ^{3}He, including nuclear relaxation studies [1, 4], polarization of electrons or ions, polarized targets for nuclear physics, etc. (for a review, see for example Ref. [5]). Another motivation for creating polarized ^{3}He is the study of the quantum properties of gaseous ^{3}He↑ at low temperatures [6].

In simple optical pumping situations, in which the relevant levels are the $2J_g + 1$ and $2J_e + 1$ Zeeman sublevels of the ground and excited states, which have well defined angular momenta, it is not difficult to predict the effect of the characteristics of the pumping light (intensity, polarization or frequency) on the atomic populations. In ^{3}He, the situation is complicated by the indirect character of the optical pumping (pumping through an intermediate metastable level). As will be discussed in more detail below, this introduces non-linearities in the equation of evolution of the atomic populations. Moreover, in the metastable level there are two hyperfine sublevels which are strongly coupled by metastability exchange collisions [7]. Finally the fine and hyperfine structures of the upper level of the optical transition, the 2 ^{3}P level, are comparable; as a consequence, the role of the 9 fine and hyperfine components of the 2 ^{3}S-2 ^{3}P transition at $\lambda = 1.08\ \mu$ has to be studied in detail.

The aim of this article is to discuss a model which allows a numerical calculation of the nuclear polarization as a function of the intensity and polarization of the optical pumping source on each of the 9 components of the $\lambda = 1.08\ \mu$ line. The model incorporates exactly the effect of the metastability exchange collisions and of the photons on the atoms, whatever the light intensity; on the other hand, it relies on strong approximations to study the collisional redistribution of velocities and populations inside both

$2\,^3S$ and $2\,^3P$ states. The present work is a generalization of that of Timsit and Daniels [8], who considered optical pumping with circularly polarized resonance radiation from a ^4He discharge light source. Such a generalization is justified by the much higher flexibility offered by a laser which can be tuned on any of the components of the $\lambda = 1.08\ \mu$ line [9]. Moreover, the present calculations include stimulated emission, which was not the case in previous studies.

A comparison of the calculations with experimental results is presented, both for room temperature and low temperature situations, where the kinetics parameters are different.

1. Kinetics of optical pumping in ^3He.

1.1 NOTATION. — The $1\,^1S_0$ ground level of ^3He has two nuclear magnetic sublevels, $m_I = \pm 1/2$. Their relative populations are denoted $(1 \pm P)/2$, where P is the nuclear polarization $(-1 \leqslant P \leqslant 1)$. The excited $2\,^3S_1$ state is split into two hyperfine sublevels ($F = 3/2$ and $1/2$) which are in turn split into 6 magnetic sublevels; the hyperfine structure is of the order of 6.7 GHz [10]. We call A_1, A_2, A_3 and A_4 the sublevels $m_F = 3/2$, $1/2$, $-1/2$ and $-3/2$ of the $F = 3/2$ hyperfine level of the $2\,^3S_1$ (see Fig. 1). A_5 and A_6 refer to the $m_F = 1/2$ and $-1/2$ sublevels of the $F = 1/2$ hyperfine level. Let us call a_i the number density for the metastable atoms in the A_i state.

The $2\,^3P$ level of ^3He has a more complex structure, resulting from fine and hyperfine interactions, which have been accurately measured [11-13]. It involves 5 energy levels labelled P_0, P_x, P_1, P_y and P_2 for decreasing energies (see Fig. 1). Each of them has a given value of F', ranging from 1/2 to 5/2, resulting altogether in 18 Zeeman sublevels, called B_j (j between 1 an 18). For instance B_1 refers to the $F' = 5/2$, $m'_F = 5/2$ sublevel of the P_2 level and B_{18} to the $F' = 1/2$, $m'_F = -1/2$ sublevel of the P_0 level. The correspondence between the B_j notation and the F', m'_F quantum numbers is shown in figure 1. Let us call b_j the atom number density in the B_j state. The sum

$$\sum_{j=1}^{18} b_j$$

is the total number of atoms per cm^3 in the $2\,^3P$ state.

The $2\,^3S$-$2\,^3P$ transition has 9 components, labelled C_k and shown in figure 2a. C_1 corresponds to the smallest energy difference, namely to the $(2\,^3S_1,\ F = 1/2) \rightarrow (2\,^3P_y,\ F' = 3/2)$ transition, whereas C_9 refers to the largest energy difference, namely to the $(2\,^3S_1,\ F = 3/2) \rightarrow (2\,^3P_0,\ F' = 1/2)$ transition. The structure of the $2\,^3S$-$2\,^3P$ line with the relative intensities of the 9 components is shown in figure 2b.

1.2 METASTABILITY EXCHANGE. — Here we use the treatment of metastability exchange collisions given by Partridge and Series [14], which is the starting point of the more detailed calculation of reference [7].

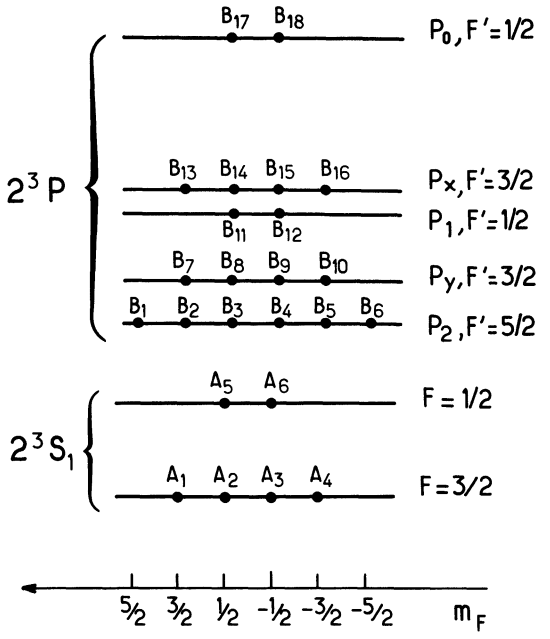

Fig. 1. — Scheme of the magnetic sublevels of the $2\,^3S_1$ and of the $2\,^3P$ states of helium 3. The correspondence is shown between the (F, m_F) quantum numbers and the i index (i between 1 and 6) for the $2\,^3S_1$ sublevels, as well as between the (F', m'_F) numbers and the j values (j between 1 and 18) for the $2\,^3P$ state.

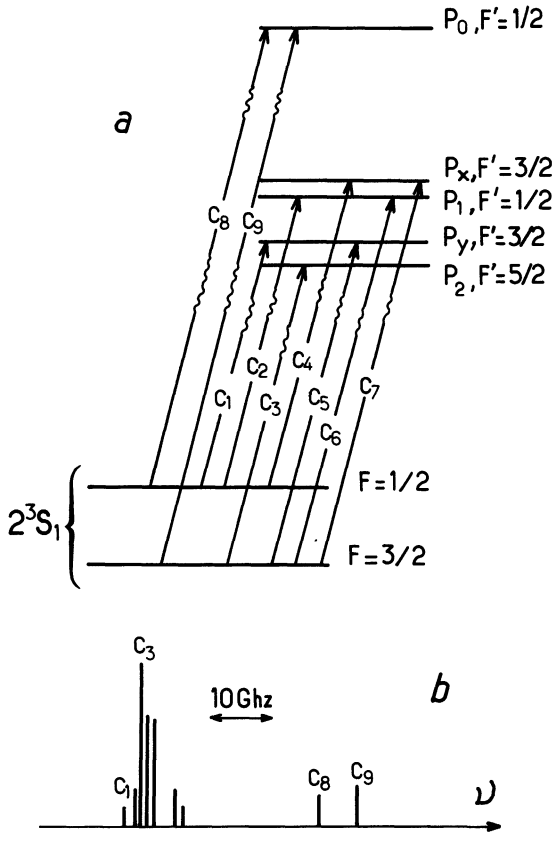

Fig. 2. — Structure of the $2\,^3S_1$-$2\,^3P$ line of ^3He. Definition of the C_k components of the line (k between 1 and 9). Figure 2a shows the relative position of the levels in energy (not to scale), figure 2b the relative position of the C_k components and their oscillator strength.

If σ_e is the metastability exchange cross-section, the exchange times T_e for the ground state and τ_e for the metastable state are given by :

$$\frac{1}{T_e} = \langle \sigma_e v \rangle n_m \quad (1)$$

$$\frac{1}{\tau_e} = \langle \sigma_e v \rangle N_g \quad (2)$$

where the brackets denote thermal averages, N_g and n_m the number densities of ground state and metastable atoms respectively $\left(n_m = \sum_i a_i\right)$. For a gas at one torr at room temperature, typical values in good optical pumping conditions are :

$$T_e \simeq 1\,\text{s}, \quad \tau_e \simeq 10^{-6}\,\text{s}.$$

We assume, as in [14], that :

(i) The internal (spin) and external (velocity) variables of the atoms are not correlated. We shall come back to this assumption and modify it : clearly, it is not fully justified for a highly monochromatic laser excitation which is velocity selective and constantly introduces correlations between internal and external atomic variables.

(ii) Neither the nuclear nor the electronic spins are affected by metastability exchange collisions, which are very fast processes. This is a very good approximation (Wigner spin rule), that has been checked experimentally in [7].

(iii) The rate of metastability exchange collisions is negligible when compared to the hyperfine frequency inside the 2 ^{3}S metastable level. Then, the off diagonal elements of the density matrix between the two $F = 1/2$ and $3/2$ hyperfine sublevels remain negligible (secular approximation).

The evolution of the density operator ρ_g (in the ground level) and ρ_m (in the metastable level) is given by :

$$\frac{1}{dt}\rho_g = \frac{1}{T_e}(-\rho_g + \text{Tr}_e\,\rho_m) \quad (3)$$

$$\frac{1}{dt}\rho_m = \frac{1}{\tau_e}\left\{-\rho_m + \sum_{F=1/2,F=3/2} P_F(\rho_g \otimes \text{Tr}_n\,\rho_m)\,P_F\right\} \quad (4)$$

where Tr_e, Tr_n are trace operators over the electronic and nuclear variables respectively, P_F the projector on the hyperfine F substate of the 2 $^3S_1$ state.

In [7], the non-linear equations of evolution of the hyperfine populations, orientations and alignment under the effect of metastability exchange collisions were derived. Here, it is more convenient to use a different basis and to write the evolution of each separate population a_i directly (this is mainly because we wish to write the effects of optical excitation in detail). Actually, the partial trace in (4) is more easily obtained in yet another basis (the decoupled $|\, m_I\, m_S \rangle$ basis), but it is simple to use Clebsch-Gordon coefficients to go to a coupled $|\, F m_F \rangle$ basis. Equations (3) and (4) then become :

$$\frac{d}{dt}a_i = (1/\tau_e)\sum_l (E_{il}\,a_l + F_{il}\,a_l\,P) \quad (5)$$

$$\frac{d}{dt}P = (1/T_e)[-P + \langle I \rangle_m] \quad (6a)$$

where

$$\langle I \rangle_m = \left(\sum_i \lambda_i a_i\right)\Big/\sum_i a_i. \quad (6b)$$

The elements of the 6 × 6 matrices E and F are given in table I, as well as the coefficients λ_i.

The physical meaning of equations (6) is clear : collisions transfer $\langle I \rangle_m$ the nuclear polarization of the metastable state to the ground state. Equations (5), which rule the evolution of the a_i's, are linear if P is fixed, that is one time scales too short for the ground state polarization to evolve (time $\ll T_e$). On the other hand, on longer time scales, they are clearly not linear. The quadratic term in equation (5) comes from the cross-term in equation (4) for the density matrices and results from the coupling introduced by exchange collisions between the ground state nuclear polarization and the metastable electronic orientation.

On equations (5) and (6) one can check that if :

$$a_1/a_2 = a_2/a_3 = a_3/a_4 = (1 + P)/(1 - P)$$

Table I. — *In this table the matrix elements of equations* (5) *and* (6) *in the text are calculated, referring to the evolution of atomic populations in the* 2 $^3S_1$ *and* 1 $^1S_0$ *states under the effect of metastability exchange collisions. Matrix E rules the linear terms in the rate equations, matrix F the non-linear terms.*

$$E = \frac{1}{18}\begin{pmatrix} -9 & 3 & 0 & 0 & 6 & 0 \\ 3 & -13 & 4 & 0 & 4 & 2 \\ 0 & 4 & -13 & 3 & 2 & 4 \\ 0 & 0 & 3 & -9 & 0 & 6 \\ 6 & 4 & 2 & 0 & -13 & 1 \\ 0 & 2 & 4 & 6 & 1 & 3 \end{pmatrix}$$

$$F = \frac{1}{18}\begin{pmatrix} 9 & 3 & 0 & 0 & 6 & 0 \\ -3 & 3 & 4 & 0 & 0 & 2 \\ 0 & -4 & -3 & 3 & -2 & 0 \\ 0 & 0 & -3 & -9 & 0 & -6 \\ -6 & 0 & 2 & 0 & -3 & 1 \\ 0 & -2 & 0 & 6 & -1 & 3 \end{pmatrix}$$

$$\lambda = \frac{1}{3}\begin{pmatrix} 3 & 1 & -1 & -3 & -1 & +1 \end{pmatrix}$$

and

$$a_2 = a_5 \quad (m_F = 1/2 \text{ sublevels})$$

$$a_3 = a_6 \quad (m_F = -1/2 \text{ sublevels})$$

the time derivative of each a_i vanishes. The reason for this is discussed in [3] : as in spin-exchange collisions between different alkalies, the polarization of one species (here the polarization P of the ground state) behaves for the other species (the metastable atoms) as a « spin temperature », which assigns an exponential m_F dependence to the populations.

1.3 Coupling to the radiation field.

1.3.1 *Absorption probabilities.* — A monochromatic pumping field can be written :

$$\mathbf{E} = \mathbf{e}_\lambda \mathcal{E} e^{i\omega t} + \mathbf{e}_\lambda^* \mathcal{E} e^{-i\omega t} \tag{7}$$

($\mathcal{E}$ is a real number).

The laser frequency is $\omega/2\pi$, its polarization vector $\mathbf{e}_\lambda$ and its intensity I/S per surface unit :

$$I/S = 2\varepsilon_0 c\mathcal{E}^2 \tag{8}$$

(I/S is expressed in watt $\times$ m^{-2}).

Let us calculate the absorption rate $1/\tau_{ij}$ of laser photons by the metastable atoms. τ_{ij} refers here to a transition taking place between the (F, m_F) substate A_i of the $2\,^3S_1$ level (of population a_i) and the (F', m'_F) substate B_j of the $2\,^3P$ level (of population b_j). This probability $1/\tau_{ij}$ is given by :

$$1/\tau_{ij} = \frac{q^2}{\hbar^2}\mathcal{E}^2 \frac{\Gamma'}{(\Gamma'/2)^2 + (\omega - \omega_k)^2} |\langle A_i | \mathbf{e}_\lambda \cdot \mathbf{R} | B_j \rangle|^2 \tag{9}$$

where q is the electron charge and $\Gamma'/2$ the damping rate of the optical coherence between the $2\,^3S_1$ and $2\,^3P$ states.

$q\mathbf{R}$ is the optical dipole operator acting between the atomic states A_i and B_i, $(\omega - \omega_k)/2\pi$ is the frequency difference between the laser and the transition corresponding to the kth component of the atomic line.

The absorption probability can be written :

$$1/\tau_{ij} = \gamma_k T_{ij} \tag{10}$$

where γ_k is a coefficient which contains all the laser characteristic dependences, whereas T_{ij} is the transition matrix element between the sublevels A_i and B_j. The calculation of the T_{ij} coefficients is given in section 1.3.3. It implies the knowledge of the structure of the $2\,^3P$ level of helium 3, resulting from comparable fine and hyperfine interactions. We first calculate the eigenvectors of the Hamiltonian in the $2\,^3P$ state and then all the T_{ij} elements given in table III.

1.3.2 *Structure of the* $2\,^3P$ *level.* — The ^4He atom in the $2\,^3P$ state has 3 levels of $J' = 0$, 1 and 2 between which the energy splittings are given in references

Table II. — *In the first columns of table* IIa *the values of the* x_1, x_2 *coefficients occurring in formula* (11) *of the text* (§ 1.3.2) *are listed. They refer to the mixing of different* J' *values for each of the* F' *hyperfine levels of the* $2\,^3P$ *state of helium* 3. *The third column of table* IIa *shows the energy of each level. Table* IIb *shows the energy splitting of the* C_k *components of the* $2\,^3S_1$-$2\,^3P$ *transition.*

Table IIa.

Level	x_1	x_2	Energy (GHz)
P_0	0.994	− 0.109	0
P_x	0.553	− 0.833	− 27.39
P_1	0.109	0.994	− 28.13
P_y	0.833	0.553	− 32.64
P_2	1	0	− 34.41

Table IIb

Transition C_k	Energy difference (GHz)
C_1	0
C_2	4.51
C_3	4.97
C_4	5.25
C_5	6.74
C_6	11.25
C_7	11.99
C_8	32.64
C_9	39.38

Table III. — *Transition matrix elements* T_{ij} *for each of the* 9 C_k *components of the* $2\,^3S$-$2\,^3P$ *line of* ^3He. *Each column refers to a given* A_i *sublevel of the* $2\,^3S_1$ *state, each line to a given* B_j *sublevel of the* $2\,^3P$ *state. For a correspondence between the i and j numbers and the quantum numbers, see figure* 1. *The polarization of the light inducing the transition* (σ^+, π *or* σ^-) *is also indicated for each* T_{ij} *probability.*

Transition C_1

j \ i	5	6
7	0.0270 (σ^+)	
8	0.0180 (π)	0.0090 (σ^+)
9	0.0090 (σ^-)	0.0180 (π)
10		0.0270 (σ^-)

Transition C_2

j \ i	5	6
11	0.1867 (π)	0.3735 (σ^+)
12	0.3735 (σ^-)	0.1867 (π)

Transition C_3

j \ i	1	2	3	4
1	1 (σ^+)			
2	0.4 (π)	0.6 (σ^+)		
3	0.1 (σ^-)	0.6 (π)	0.3 (σ^+)	
4		0.3 (σ^-)	0.6 (π)	0.1 (σ^+)
5			0.6 (σ^-)	0.4 (π)
6				1 (σ^-)

Transition C_4

j \ i	5	6
13	0.9729 (σ^+)	
14	0.6486 (π)	0.3243 (σ^+)
15	0.3243 (σ^-)	0.6484 (π)
16		0.9729 (σ^-)

Transition C_5

j \ i	1	2	3	4
7	0.5837 (π)	0.3892 (σ^+)		
8	0.3892 (σ^-)	0.0648 (π)	0.5189 (σ^+)	
9		0.5189 (σ^-)	0.0648 (π)	0.3892 (σ^+)
10			0.3892 (σ^-)	0.5837 (π)

Transition C_6

j \ i	1	2	3	4
11	0.2198 (σ^-)	0.1466 (π)	0.0733 (σ^+)	
12		0.0733 (σ^-)	0.1466 (π)	0.2198 (σ^+)

Transition C_7

j \ i	1	2	3	4
13	0.0162 (π)	0.0108 (σ^+)		
14	0.0108 (σ^-)	0.0018 (π)	0.0144 (σ^+)	
15		0.0144 (σ^-)	0.0018 (π)	0.0108 (σ^+)
16			0.0108 (σ^-)	0.0162 (π)

Transition C_8

j \ i	5	6
17	0.1465 (π)	0.2931 (σ^+)
18	0.2931 (σ^-)	0.1465 (π)

Transition C_9

j \ i	1	2	3	4
17	0.2801 (σ^-)	0.1867 (π)	0.0934 (σ^+)	
18		0.0934 (σ^-)	0.1867 (π)	0.2801 (σ^+)

[11, 12] and [13]. J' is no longer a « good » quantum number in the case of ^{3}He, in which the hyperfine coupling mixes levels of the same F' quantum number but different values of J' (1), namely $J' = F' - 1/2$ and $J' = F' + 1/2$.

The hyperfine Hamiltonian, due to contact interaction between the nuclear spin **I** and the spin **S** of the 1s electron, can be written in the form $A\,\mathbf{I}\cdot\mathbf{S}$, with $A = -4.33$ GHz [13, 15]. Expressing the Hamiltonian in the $|\,I(L'S')J'F'm'_F\rangle$ basis leads for the $2\,^3$P state to a 5×5 symmetrical non-diagonal matrix, whose eigenvalues are the energies of the 5 levels labelled P_0, P_x, P_1, P_y and P_2 in figure 2a (not to scale).

Levels P_0 and P_1 have $F' = 1/2$ and they are admixtures of $J'_1 = 0$ and $J'_2 = 1$. Levels P_x and P_y have $F' = 3/2$ and are admixtures of $J'_1 = 1$ and $J'_2 = 2$. Level P_2 has $F' = 5/2$ and $J' = 2$. For the 4 levels corresponding to two different J' values, one can write the eigenvectors in the following way :

$$|\,2\,^3\mathrm{P}, F'\rangle = x_1\,|\,J'_1, F'\rangle + x_2\,|\,J'_2, F'\rangle \qquad (11)$$

with $x_1^2 + x_2^2 = 1$.

The values of the (x_1, x_2) sets of parameters are listed in table IIa. Level P_0 has only a small contribution of $J' = 1$; in the same way, level P_1 has only a small fraction of $J' = 0$, whereas for P_x and P_y no approximate value of J' can be assigned. The energy differences between the 5 levels are also listed in table IIa. Table IIb shows the energy splitting between the C_k components of the $2\,^3S_1$-$2\,^3P$ line.

1.3.3 *Transition matrix elements.* — Let us evaluate the angular dependence of the transition probability :

$$T_{ij} = \beta\,|\langle \mathrm{A}_i\,|\,\mathbf{e}_\lambda\cdot\mathbf{R}\,|\,\mathrm{B}_j\rangle|^2 \qquad (12)$$

where β is a coefficient independent of the A_i, B_j sublevels involved in the transition.

T_{ij} is given by :

$$T_{ij} = \beta\begin{pmatrix} F & 1 & F' \\ -m_F & \delta & m'_F\end{pmatrix}^2 |\langle 2\,^3S_1, F \,\|\, R \,\|\, 2\,^3P, F'\rangle|^2 \qquad (13)$$

with : $\delta = m'_F - m_F$.

($\delta = 1, 0$ and -1 respectively for σ^+, π, and σ^- polarizations of the light.) Let us now express the $|\,2\,^3P, F'\rangle$ kets in a decoupled basis. The $|\,2\,^3P, F'\rangle$ states being mixtures of different J' (see formula (11)), one can write :

$$\frac{|\langle 2\,^3S_1, F \,\|\, R \,\|\, 2\,^3P, F'\rangle|^2}{(2F+1)(2F'+1)} = x_1^2\begin{Bmatrix} 1 & 1 & J'_1 \\ F' & 1/2 & F\end{Bmatrix}^2 |\langle 2\,^3S_1 \,\|\, R \,\|\, 2\,^3P, J'_1\rangle|^2 +$$

$$+ x_2^2\begin{Bmatrix} 1 & 1 & J'_2 \\ F' & 1/2 & F\end{Bmatrix}^2 |\langle 2\,^3S_1 \,\|\, R \,\|\, 2\,^3P, J'_2\rangle|^2 +$$

$$+ 2x_1x_2\begin{Bmatrix} 1 & 1 & J'_1 \\ F' & 1/2 & F\end{Bmatrix}\begin{Bmatrix} 1 & 1 & J'_2 \\ F' & 1/2 & F\end{Bmatrix}\langle 2\,^3S_1 \,\|\, R \,\|\, 2\,^3P, J'_1\rangle\langle 2\,^3S_1 \,\|\, R \,\|\, 2\,^3P, J'_2\rangle. \qquad (14)$$

One can calculate the matrix elements in the decoupled basis :

$$\langle 2\,^3S_1 \,\|\, R \,\|\, 2\,^3P, J'\rangle = 3(2J'+1)\begin{Bmatrix} 0 & 1 & 1 \\ J' & 1 & 1\end{Bmatrix}^2 |\langle 2\,^3S_1 \,\|\, R \,\|\, 2\,^3P\rangle|^2. \qquad (15)$$

Relative values of the T_{ij} coefficients can be calculated using equations (13), (14), (15) and (11). They are listed in table III for each of the 9 C_k components.

Each lower level A_i can be connected to 3 upper levels B_j, corresponding to $m'_F - m_F = +1, 0$ and -1 respectively for σ^+, π and σ^- polarizations of light. All T_{ij} coefficients range between 0 and 1 and have been normalized so that :

$$T_{11} = \frac{\beta}{3}|\langle 2\,^3S_1 \,\|\, R \,\|\, 2\,^3P\rangle|^2 = 1.$$

In order to calculate the β proportionality coefficient of formula (12), let us evaluate the reduced matrix element appearing in formula (15) in terms of the total oscillator strength f of the $2\,^3S_1$-$2\,^3P$ transition (see Appendix A) :

$$|\langle 2\,^3S_1 \,\|\, R \,\|\, 2\,^3P\rangle|^2 = \frac{3\hbar}{2m\omega}f = \frac{3}{\beta}. \qquad (16)$$

This finally allows us to calculate the absorption probability $1/\tau_{ij}$; its laser dependent part γ_k (see formula (10)) can be written, using (8), (9), (12) and (16) :

$$\gamma_k = \frac{4\pi\alpha f(I/S)}{m\omega\Gamma'} \times \frac{\Gamma'^2/4}{(\Gamma'^2/4) + (\omega - \omega_k)^2}. \qquad (17)$$

(1) For ^{3}He the notation J' has no real physical meaning, but is defined by continuity from the ^{4}He case : J' stands only for the total momentum that one would ascribe to the level if the hyperfine coupling was infinitely small.

1.4 TOTAL EQUATIONS OF EVOLUTION.

1.4.1 *Correlations between internal and external variables.* — We now come back to an assumption made earlier, namely that there is no correlation between atomic velocities and internal variables. Obviously, the velocity selective character of the laser optical pumping [16, 17] tends to create such correlations which, on the other hand, are constantly destroyed by collisions.

The metastable atoms mainly undergo two kinds of collisions :

(i) Direct collisions with no metastability exchange. Such collisions have very little effect on the internal variables of atoms (**I** and **S**); a good approximation is to consider them as true velocity changing collisions. Small velocity changes, corresponding to large impact parameters, have a relatively large probability. Such collisions tend to equalize the orientations of different velocity classes.

(ii) Metastability exchange collisions which exchange the nuclear polarization of the ground and metastable atoms, but do not affect the electronic orientation **S** of the metastable atoms. These collisions, with resonant energy transfer, require some overlap between the electronic orbitals and therefore occur at relatively small impact parameters. The incoming and outgoing metastable atoms, having rather different velocities, can still have their orientations coupled through the conservation of **S**.

The effect of the pumping is to force an orientation larger than that of the ground state for the velocity class in resonance with the laser. If the direct collision processes (i) were dominant, the pure velocity changes would destroy any correlation between internal and external variables. All the metastable atoms would be polarized in the same way. Actually, in most experimental situations, this does not occur and exchange collisions (ii) force an orientation closer to that of the ground state for the metastable atoms having a velocity very different from the velocity in resonance with the laser.

A realistic treatment of the problem would include a separate study of all velocity classes, and require a knowledge of the collision kernel for each type of collision. This is too complicated and we shall here use a simple model : the metastable atoms are merely divided into two groups. The first group, with total number density n_m^* and state populations a_i^*

$$\left(\sum_i a_i^* = n_m^*\right),$$

is effectively oriented by the laser. It includes atoms in resonance with the laser and atoms with slightly different velocities, which are coupled very rapidly to the former by non-depolarizing velocity changing collisions. The second group, with total number density $n_m - n_m^*$ and populations $a_i - a_i^*$, is supposed not to interact in any way with the laser, so that its only role is to contribute through metastability exchange to the nuclear relaxation of the ground state [1, 18] ([2]). Actually, this model is not completely realistic, because the limit between the two groups is not physically well defined. However, it has the advantage of taking into account the correlations between orientations and velocities with only one parameter n_m^*/n_m. This is reasonable as long as one is only interested in the nuclear polarization in the ground state, which averages the details of the effects occurring in the metastable level.

As a consequence, equation (5) still holds for the populations of both classes of metastable atoms, namely a_i^* and $(a_i - a_i^*)$, and equation (6) can be written

$$\frac{dP}{dt} = \frac{1}{T_e}\left[-P + \frac{1}{n_m}\sum_i \lambda_i (a_i - a_i^*) + \frac{1}{n_m}\sum_i \lambda_i a_i^*\right]. \tag{18}$$

There are also some changes to be made in the equations derived in section 1.3 for the coupling of the metastable atoms to the radiation field. Equations (10) and (17) give the probability of photon absorption by one velocity class of the metastable atoms, corresponding to the frequency $\omega_k/2\pi$ close to the laser frequency $\omega/2\pi$. This result should be extended to the ensemble of metastable atoms of density n_m^* considered above. This means that the γ_k coefficients are to be integrated over frequency in a domain corresponding to the velocity spread of the n_m^* atoms. Equation (10) is thus to be replaced by

$$1/\tau_{ij} = \bar{\gamma}_k T_{ij} \tag{19}$$

where γ_k is replaced by a mean value $\bar{\gamma}_k$, for which a calculation is given in appendix B, assuming that the kernel of the velocity changing collisions is much larger than Γ', the absorption profile of the laser by the atoms. This condition is equivalent to

$$D(n_m^*/n_m) \gg \Gamma'/2\pi \tag{20}$$

where D is the Doppler width of the metastable velocity distribution. We shall see later that the inequality (20) is valid at any temperature of interest for this article. Under this condition, $\bar{\gamma}_k$ can be written, according to formula (B2) of appendix B :

$$\bar{\gamma}_k = \sqrt{\frac{\pi}{2}}\,\frac{\alpha f(I/S)(n_m/n_m^*)}{m\omega D}\exp[-(\omega - \omega_k^0)^2/(2\pi D)^2]. \tag{21}$$

([2]) In such a picture nf the n_m^* effectively orientated atoms, the model given above does not take into account the coupling between the 2 groups of metastable atoms due to the conservation of **S** during exchange collisions. However, if one gives up this simple picture of the n_m^* atoms, one could define a group of n_m^* effectively pumped atoms in such a way that the above coupling is included, at least partially.

The exponential factor in formula (21) is only to be considered when the laser frequency $\omega/2\pi$ is mistuned from the transition frequency $\omega_k^0/2\pi$ for atoms at rest ([3]).

1.4.2 *Relaxations.* — Up to this point only coupling with photons and metastability exchange collisions have been considered. They are the processes that can be exactly calculated from a microscopic point of view. However, other collisional processes not yet taken into account can relax the atomic orientations in each of the 3 levels involved in the kinetics of ^{3}He optical pumping.

The nuclear orientation of the ground state atoms in a ^{3}He discharge can be destroyed by various kinds of collisions (wall collisions, collisions with electrons, ions, molecules, etc.). Without trying to describe them all, one just assumes a unique relaxation time T_r acting on the ground state orientation as follows :

$$\frac{d}{dt}P = -\frac{1}{T_r}P. \tag{22}$$

In practice T_r is of the order of 1 min (much shorter than in the absence of a discharge).

The metastable atoms are also affected by many kinds of collisions. In addition to metastability exchange, already discussed in section 1.2, collisions with the species present in a discharge plasma may transfer atoms from a state A_i to a different state A_k, or even make them lose their excitation. Moreover, collisions with the walls of the sample are very likely to de-excite them; since their total number is constant, it means that they are replaced by newly excited atoms in unrelated states, which amounts to a relaxation process. We will not try here to give a detailed description of the relaxation in the metastable level, because we have no quantitative knowledge of all the relevant processes. We will simply make the crude assumption that each population is relaxed towards an average value with a rate $1/\tau_r$:

$$\left.\begin{aligned} &\frac{d}{dt}a_i^* = \frac{1}{\tau_r}\left(\sum_k \frac{a_k^*}{6} - a_i^*\right) \\ &\text{and} \\ &\frac{d}{dt}(a_i - a_i^*) = \frac{1}{\tau_r}\left[\sum_k \frac{(a_k - a_k^*)}{6} - (a_i - a_i^*)\right] \end{aligned}\right\} \tag{23}$$

Such a description is in fact not necessarily irrealistic, especially if the pressure is low so that the dominant relaxing process comes from collisions with the walls.

In the same way, atoms in the 2 ^{3}P level can be transferred from a B_j to a B_l state by collisions during their radiative lifetime, at a significant rate if the pressure is high enough. These processes have not been calculated or measured for ^{3}He. So, in order to take them into account, at least crudely, we will introduce an *ad hoc* average relaxation rate $1/\tau_{dep}$ such that :

$$\frac{db_j}{dt} = \frac{1}{\tau_{dep}}\left[\sum_l \frac{b_l}{18} - b_j\right]. \tag{24}$$

In this description, the choice of values for τ_{dep} which are very long or very short (compared to the radiative lifetime τ) will allow us to describe correctly the low pressure limit (where collisions are unfrequent) and the high pressure regime (in which one can assume a total redistribution between the B_j states through collisions).

1.4.3 *Final equations.* — Let us now add up the effects of all the processes above mentioned and derive the coupled equations of evolution for all the levels involved in the optical pumping process.

For the atoms in the A_i state that are not affected by the laser, one simply has :

$$\frac{d}{dt}(a_i - a_i^*) = (1/\tau_r)\left[\sum_k \frac{a_k - a_k^*}{6} - (a_i - a_i^*)\right] + \\ + (1/\tau_e)\sum_k [(E_{ik} + PF_{ik})(a_k - a_k^*)]. \tag{25}$$

For atoms pumped by the laser, one has in addition the effect of the absorption of photons (with a rate $1/\tau_{ij}$, given by (19)) and of spontaneous and stimulated emissions from the 2 ^{3}P state :

$$\frac{d}{dt}a_i^* = (1/\tau_r)\left[\sum_k \frac{a_k^*}{6} - a_i^*\right] + \\ + (1/\tau_e)\sum_k [E_{ik} + PF_{ik}]\, a_k^* \\ + \sum_j (1/\tau_{ij})(b_j - a_i^*) + (1/\tau)\sum_j T_{ij}\, b_j. \tag{26}$$

In the same way the evolution of the populations of each state B_j of the 2 ^{3}P level can be written :

$$\frac{d}{dt}b_j = -\frac{b_j}{\tau} + \sum_i \frac{1}{\tau_{ij}}(a_i^* - b_j) + \frac{1}{\tau_{dep}}\left[\sum_l \frac{b_l}{18} - b_j\right]. \tag{27}$$

Finally, the evolution of the ground state polarization is given by

$$\frac{d}{dt}P = -\frac{P}{T_r} + \frac{1}{T_e}\left[-P + \frac{1}{n_m}\sum_i \lambda_i(a_i - a_i^*) + \right. \\ \left. + \frac{1}{n_m}\sum_i \lambda_i\, a_i^*\right]. \tag{28}$$

2. Numerical and experimental results.

2.1 METHOD USED TO SOLVE THE EQUATIONS. — Equations (25), (26), (27) and (28) obtained in the preceding section rule the time evolution of all the popula-

([3]) The Doppler profile has a Gaussian shape only over a few Doppler widths. The exact shape is a Voigdt profile.

tions that play a part in the mechanism of optical pumping. To solve them, we shall use the fact that the characteristic time constants are very different for the populations of the excited states and for the polarization of the ground state : from (28) we deduce that the time scale for the evolution of P is T_e or T_r, of the order of seconds, whereas (25), (26) and (27) show that for any fixed value of P, the a_i's, the a_i^*'s and the b_i's will reach a steady value in times of the order of τ_e or τ, i.e. in microseconds. Thus, as long as we are interested only in the steady state populations of the excited states, we can take P as a parameter in (26) ; the a_i's and b_i's are simply the solutions of the set of linear coupled equations obtained from (26) and (27), replacing the time derivatives on the left hand side by zero.

This is a set of 24 equations with 24 variables, but these equations are not independent; since all the processes taken into account in this model (absorption and emission of photons, depolarizing collisions) can just transfer an atom from a given state A_i or B_j to another one, the total number of atoms in both excited states, namely $n = \sum_i a_i^* + \sum_j b_j$, is constant. This number n is fixed by the characteristics of the discharge that populates the metastable level. For small values of P and low laser powers, n is simply n_m^*, but this may become untrue in a polarized plasma : various processes (e.g. metastable-metastable Penning collisions [19]) that determine the regime of a discharge may depend on the polarizations of both the ground state and the excited state, thus causing the metastable population $\sum_i a_i^*$ to vary with P. Moreover, for high laser powers, the total population of the $2\,^3P$ state may become significant, since a saturating transition between A_i and B_j populates the B_j state up to $b_j \simeq a_i^*$. However, for the sake of simplicity we shall assume here that

$$\sum_i a_i^* + \sum_j b_j = n_m^* \qquad (29)$$

and come back to this assumption in section 2.

Solving any 23 of these 24 equations together with (29) will give a unique solution for the a_i^*'s and b_j's, for any value of the following parameters : nuclear polarization P, laser characteristics τ_{ij}, exchange time τ_e, effective metastable density n_m^* and relaxation times. In much the same way, P being a parameter in (25), one can solve the set of 6 equations for the six variables $(a_i - a_i^*)$ by solving any five of them with the additional condition : $\sum_i (a_i - a_i^*) = n_m - n_m^*$, for which the same assumptions are made as for (29). Using these solutions in (28), one gets the time derivative of P for any given value of P. A numerical integration then gives the build-up of the polarization as a function of time. If one is only interested in stationary values for P, they can be easily computed by a trial and error method : all the results presented in this paper were obtained in this way. Using standard algorithms and a fast microcomputer, it takes a few seconds to get P for a set of parameters.

2.2 CHOICE OF PARAMETERS FOR THE MODEL. — Numerical results from the above model require a choice of the parameters in equations (25) to (28) corresponding to realistic situations. Some of them can be found in published results and others were measured in our experiment; the remaining ones were let free.

The exchange rate $1/\tau_e$, for a given density N_g of the helium gas, depends strongly on the relative velocity of the colliding atoms [20]. The exchange time τ_e thus varies with temperature. From [20], if $N_g = 3.2 \times 10^{16}$ cm^{-3} (density at 1 torr and room temperature), one obtains :

$$\tau_e = 2.2 \times 10^{-6}\ \text{s} \quad \text{at} \quad 300\ \text{K}$$
$$\tau_e = 3.5 \times 10^{-5}\ \text{s} \quad \text{at} \quad 77\ \text{K}$$
$$\tau_e = 3.5 \times 10^{-4}\ \text{s} \quad \text{at} \quad 4.2\ \text{K}.$$

The decay time constant τ from the $2\,^3P$ state through spontaneous emission can be derived from the oscillator strength f of the transition $2\,^3S$-$2\,^3P$. With the values of reference [24], one obtains (see Appendix A) :

$$f = 0.5391$$
$$\tau = 0.978 \times 10^{-7}\ \text{s}.$$

For other time constants occurring in equations (25) to (28), such as T_e, T_r and τ_r, we performed additional experiments with our ^{3}He optical pumping set-up, which is described elsewhere [21]. T_e is related to τ_e by equations (1) and (2) which involve n_m, the total density of metastable atoms. To evaluate n_m, we sent a weak laser probe beam through the cell and measured its absorption by the discharge; the laser was operated in single mode and its frequency could be tuned over the Doppler absorption profile of any of the C_k components. From these measurements we deduced n_m, which of course strongly depends on the discharge level; for the very weak discharges that one uses for optimal nuclear polarizations, n_m was of the order of 2×10^{10} cm^{-3} at 300 K and hardly depended on temperature.

The decay rate $1/T_r$ in equation (28) is the intrinsic relaxation rate for the ground state atoms. Experimentally, if one monitors the decay of P when the pumping light is switched off, one obtains a time constant T_1, typically of the order of 100 s. T_1 is not necessarily identical to T_r : actually $1/T_1$ is the sum of two terms, the intrinsic rate $1/T_r$ and a contribution through metastability exchange of the relaxation occurring in the $2\,^3S$ state. One can show [7] that, if $P \ll 1$, this total rate is given by :

$$1/T_1 = 1/T_r + (11/3)(1/\tau_r)(n_m/N_g). \qquad (30)$$

No attempt was made to measure the relaxation time τ_r, but (30) shows that it cannot be shorter than $\frac{11}{3} T_1 \frac{n_m}{N_g}$, and on the other hand τ_r cannot be much longer than the diffusion time to the walls of the cell, where the atoms are de-excited ([4]). In most cases those limits for τ_r are not far apart ([5]) and in the next section it will be shown that, provided T_r is set according to (30), the choice of τ_r hardly affects the results of the calculation.

Up to now all the parameters appearing in equations (25) to (28) (and those of (19) and (21) necessary to calculate $1/\tau_{ij}$) have been discussed and assigned a value, except for n_m^* and τ_{dep}. In the next section (§ 2.3) numerical results will be derived from the model for different values of n_m^* and τ_{dep}. These last two parameters will be given reasonable limiting values (for instance $n_m/100 < n_m^* < n_m$) and their influence on the results for P will be discussed. In section (2.4) the comparison between calculations and experiments will help assigning values to n_m^* and τ_{dep} corresponding to actual optical pumping situations.

2.3 NUMERICAL RESULTS. — Before giving the numerical solution of the set of non-linear equations (25) to (28) with the values of parameters found above, one can make a preliminary remark, dealing with the respective orders of magnitude of the different evolution rates ($1/\tau_e$, $1/\tau_r$, $1/\tau$, $1/\tau_{ij}$) for metastable atoms occurring in equations (25) and (26). A crucial parameter is $1/\tau_e$, because all the efficiency of the optical pumping in ^{3}He relies on the metastability exchange collisions. As seen in section 2.2, τ_e varies very much with the atomic velocities; for instance τ_e is in the microsecond range at 300 K and in the millisecond one at 4.2 K. On the other hand, the other time constants are not so much temperature dependent. This explains why, from a mathematical point of view, two different regimes can be distinguished according to the temperature :

(i) At very low temperatures ($T \lesssim 4.2$ K), τ_e is rather long. In equations (25) and (26) there are other terms much larger than the term having $1/\tau_e$ in factor, such as the term in $1/\tau_{ij}$ (as soon as the laser intensity is of the order of a few milliwatts, $1/\tau_{ij}$ is greater than $1/\tau_e$). In first approximation it is thus justified to neglect the $1/\tau_e$ term and solve the evolution equations for the metastable populations ignoring the coupling with the reservoir of ground state atoms, occurring through metastability exchange. The non-linearity of equations (25) and (26) vanishes and a solution is easily derived. In particular one can obtain the metastable nuclear polarization $\langle I \rangle_m$, given by equation (6b), for which the time constant of evolution is of the order of the shortest of all the time constants involved in equations (25) and (26) (for instance τ_{ij}). Then the nuclear polarization P of the ground state is simply calculated from (28), which reduces to :

$$\frac{d}{dt} P = -\frac{P}{T_r} + \frac{1}{T_e}[-P + \langle I \rangle_m] \qquad (31)$$

where $\langle I \rangle_m$ does not depend on P.

(ii) At high temperatures ($T = 300$ K or $T = 77$ K) τ_e is of the same order of magnitude as the other time parameters of equations (25) and (26). One can no longer neglect the coupling between metastable and ground state atoms *via* the exchange collisions. One has to solve the complete set of equations (25) to (28) without neglecting the non-linear terms in (25) and (26).

Let us first discuss the numerical results obtained at low temperatures (i), which are the most simply obtained (shown in Fig. 3).

The values of the parameters used for the model are given in the figure caption. The pumping is made either on the C_4 or C_5 components, or on both C_4 and C_5 components (denoted as $C_4 + C_5$ in Fig. 3). The dashed lines in the same figure refer to the nuclear

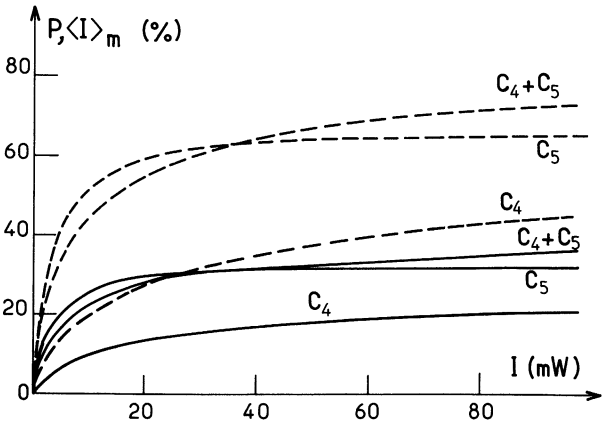

Fig. 3. — Calculated nuclear polarization of helium 3 as a function of the total intensity of the laser I (covering a surface $S = 18$ cm^2) at 4.2 K. The assumptions are : σ^+ light, $\tau_{dep} = \infty$, $n_m^*/n_m = 1$, $\tau_r = \infty$, $p = 0.3$ torr, $n_m/N_g = 2 \times 10^{-6}$, $T_1 = 100$ s. Continuous lines refer to the polarization P of the ground state, dotted lines to the nuclear polarization $\langle I \rangle_m$ of the metastable state, defined by formula (6b) in the text. The pumping is on the C_4 component, or on the C_5 one, or on both with half of the power on each one (denoted as $C_4 + C_5$).

([4]) The upper limit for the relaxation time τ_r would just be the diffusion time to the walls if one assumed a destruction of the nuclear polarization $\langle I \rangle_m$ during the de-excitation. If $\langle I \rangle_m$ is not totally destroyed, τ_r might be somewhat longer.

([5]) For instance at room temperature, for a cylindrical cell of radius $R = 2.5$ cm, length $L = 5$ cm, filled with a pressure of 0.3 torr of ^{3}He, the diffusion time to the walls for a metastable atom is 0.52×10^{-3} s [20] and $n_m/N_g \simeq 2 \times 10^{-6}$ in a weak discharge where $T_1 = 100$ s, so that $\frac{11}{3} T_1 (n_m/N_g) = 0.72 \times 10^{-3}$ s.

polarization $\langle I \rangle_m$ of the metastable state, the full lines to the nuclear polarization P of the ground state. These results show the stationary values of $\langle I \rangle_m$ and P derived from the model as a function of the laser intensity I. All these curves show a fast increase when I is in the range 1-10 mW and a saturation for higher laser intensities. The characteristics of the pumping using different components can be crudely explained : above a few tens milliwatts of σ^+ light, the $F = 3/2$ level of the metastable state is fully polarized, with nearly all its atoms in the A_1 state. However, the atoms that come to the $F = 1/2$ level by exchange or hyperfine pumping (*via* the $2\,^3P_y$ level) are not in a fully nuclear spin polarized state : altogether the nuclear polarization in the metastable state reaches a maximum.

If one tends to depopulate the metastable $F = 1/2$ level as well, for instance by pumping simultaneously with the C_4 and C_5 components, one goes slightly above the limit obtained with C_5 alone (see Fig. 3); however, pumping with C_4 alone is shown to be poorly efficient. The nuclear polarization P of the ground state follows that of the metastable state $\langle I \rangle_m$; however, P and $\langle I \rangle_m$ are not equal in this low temperature case, in which the metastability exchange is weak (the opposite result is found at high temperatures, when the metastability exchange nearly equalizes $\langle I \rangle_m$ and P). The P values for the ground state here result from the competition between metastability exchange and relaxation; with the numbers of figure 3 ($T_e = T_r = 100$ s) one obtains, from formula (31), $P = \langle I \rangle_m/2$ at all laser intensities.

Let us now present the results obtained at high temperatures (ii) (300 K and 77 K for instance), for which the use of a non-linear calculation cannot be avoided. One can first discuss the effect of the relaxation time τ_r in the metastable state. Figure 4 shows results for P at 300 K as a function of laser power pumping on the C_9 line, and the same behaviour is found whatever the pumping line. The lowest 2 curves refer to $n_m^*/n_m = 0.01$, the 2 upper ones to $n_m^*/n_m = 0.1$; the solid lines are the results for $T_r = T_1$ and $\tau_r = \infty$, the dashed lines for $T_r = \infty$ and $\tau_r = \frac{11}{3} T_1 \frac{n_m}{N_g}$. Clearly, especially if $n_m^* \ll n_m$, it is not crucial to know the exact value of τ_r as long as T_r and τ_r are set according to (30). This suggests that, as long as most of the metastable states do not contribute to the pumping ($n_m^* \ll n_m$), it is not necessary to know the detailed process of relaxation in the $2\,^3S_1$ level : the only effect relevant to the kinetics of the ground state polarization is an overall relaxation time for P. One can then disregard the $n_m - n_m^*$ atoms that do not interact with the laser, and drop the relaxation term in (26), or just as well put any reasonable value for τ_r in (25) and (26), and set T_r accordingly. On the other hand, if $n_m^* = n_m$ (this is for instance achieved at 300 K when pumping with a helium 4 discharge lamp [1]), the above discussion is not longer valid.

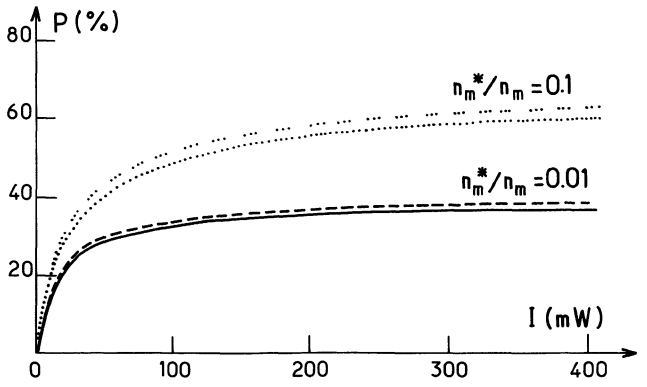

Fig. 4. — Calculated nuclear polarization P of ^{3}He ground state at 300 K as a function of total laser intensity I (on surface $S = 18$ cm^2). Assumptions : σ^+ light, laser on the C_9 component, $\tau_{dep} = \infty$, $p = 0.3$ torr, $n_m/N_g = 2 \times 10^{-6}$, $T_1 = 100$ s. Solid lines are obtained for $T_r = (11/3)\, T_1(n_m/N_g)$. One set of curves is for $n_m^*/n_m = 0.01$, the other one for $n_m^*/n_m = 0.1$.

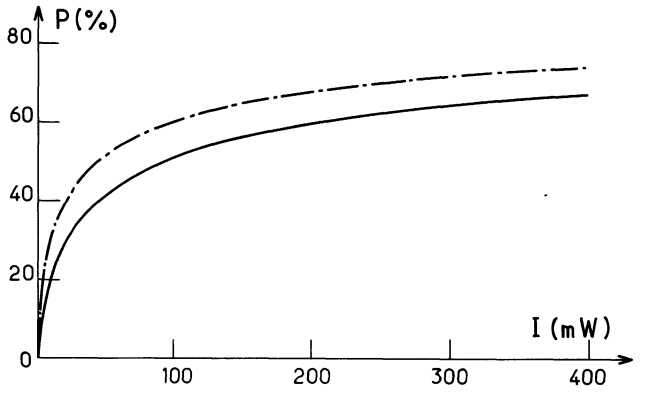

Fig. 5. — Same case as in figure 4, except that $n_m^*/n_m = 1$. Solid line : $T_r = T_1$, $\tau_r = \infty$; dotted line : $T_r = 2\,T_1$, $\tau_r = (22/3)\, T_1(n_m/N_g)$.

Figure 5 shows the calculated results for $n_m^*/n_m = 1$ in 2 cases : first $T_r = T_1$ and $\tau_r = \infty$, second $T_r = 2\,T_1$ and $\tau_r = \frac{22}{3} T_1 \frac{n_m}{N_g}$. The 2 curves are not close to each other. This is clearly due to the fact that, above a few milliwatts of pumping light, $\tau_{ij} \ll \tau_r$, which means that the relaxation of the metastable atoms is easily overriden by the pumping. In such a case, the relaxation is more efficiently overcome by the pumping if it takes place in the metastable state, directly pumped, rather than in the ground state. For accurate calculations the value of τ_r should be determined experimentally.

Let us now compare the efficiency of different pumping lines. Figure 6 shows the results in an ideal situation in which $\tau_{dep} = \infty$ (no relaxing collisions in the $2\,^3P$ state), $n_m^*/n_m = 0.1$ (reasonably efficient velocity redistribution in the $2\,^3S$ state) and $\tau_r = \infty$. Only the σ^+ polarization was used : π polarization would

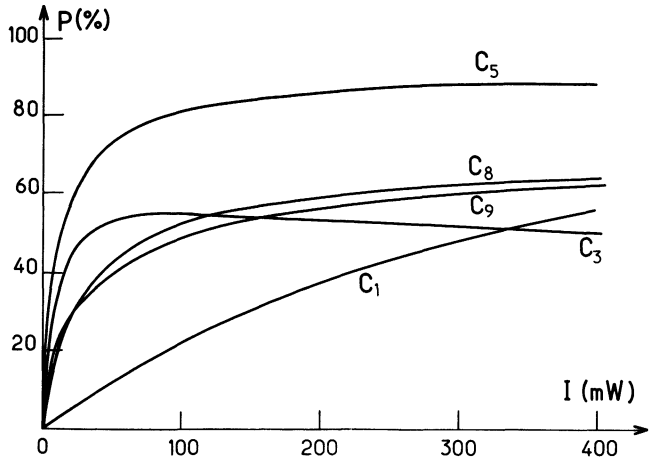

Fig. 6. — Calculated nuclear polarization P of ^{3}He as a function of laser intensity I (on $S = 18\ cm^2$) for a frequency tuned on different C_k components of the $2\ ^3S$-$2\ ^3P$ line. Calculation for 300 K, σ^+ light, $\tau_{dep} = \infty$, $n_m^*/n_m = 0.1$, $\tau_r = \infty$, $p = 0.3$ torr, $n_m/N_g = 2 \times 10^{-6}$, $T_r = T_1 = 100$ s.

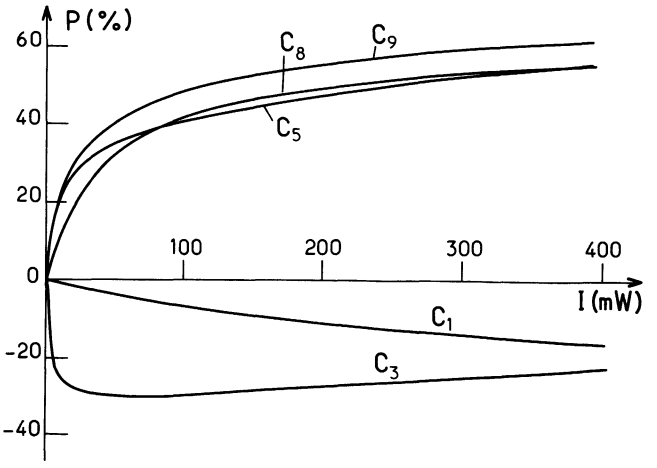

Fig. 7. — Same case as in figure 6, except that $\tau_{dep} = \tau/100$.

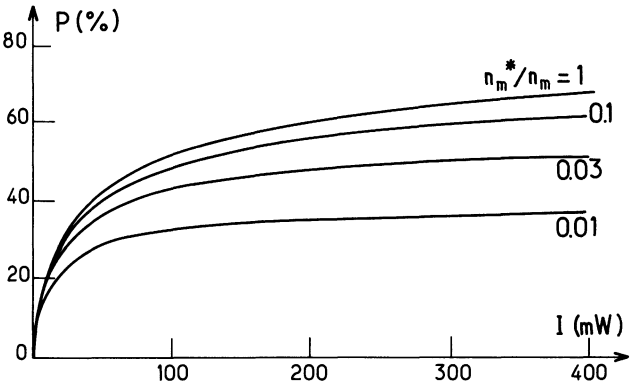

Fig. 8. — Calculated nuclear polarization P as a function of laser intensity I (on $S = 18\ cm^2$) for a frequency tuned on the C_9 component. Calculations at 300 K, σ^+ light, $\tau_{dep} = \infty$, $\tau_r = \infty$, $p = 0.3$ torr, $n_m/N_g = 2 \times 10^{-6}$, $T_r = T_1 = 100$ s. The 4 curves are for increasing values of the ratio n_m^*/n_m (0.01, 0.03, 0.1 and 1).

clearly lead to $P = 0$, and σ^- to opposite values for P. The most efficient of the lines is C_5, which is not surprising since the matrix elements for a σ^+ transition from the A_2, A_3 and A_4 states are the highest for C_5 (see Table III), allowing an efficient overpopulation of the A_1 state which is fully spin polarized. Pumping with C_3 shows a peculiar feature : above 100 mW, P decreases as the laser power increases. The remark at the end of section 1.2 shows that for high P most of the metastable atoms are in the A_1 state. Since for σ^+ transitions A_1 is a starting level only for the C_3 line (see Table III), for all transitions but C_3 the total population of the $2\ ^3P$ state will be small, namely $\sum_j b_j \ll a_1^*$ and assumption (29) is fulfilled. On the contrary, when pumping with the C_3 line at high power one has $b_1 \simeq a_1^* \simeq n_m^*/2$, so that only half of the active metastable population is left as a source of nuclear polarization for the ground state. As will be shown in figure 8 and discussed below, this leads to a lower value of P. To check this interpretation, we replaced (29) by $\sum_i a_i^* = n_m^*$ to solve the equations, and that feature disappeared for C_3, none of the other pumping curves being affected.

Figure 7 shows the effect of relaxing collisions in the $2\ ^3P$ state : here we have taken $\tau_{dep} = \tau/100$, thus forcing the equality of the populations of the sublevels in the $2\ ^3P$ state. This is rather crude, but demonstrates that collisions may play an either crucial or negligible role, depending upon the pumping line used. It is remarkable that, in this model, collisions do not affect the pumping efficiency of the C_9 component. In contrast, the effect of collisions can be drastic, up to the point where the sign of P can be reversed. This can be easily understood for the C_3 transition , since the populations of the B_j states are all equal, the A_i states produced by the radiative decay of the $2\ ^3P$ state are not polarized and the optical pumping process relies only on the depopulation of the A_i states by photon absorption. For this line, the matrix elements increase with m_F (see Table III), so that the atoms tend to accumulate in the A_4 state, whose nuclear polarization is negative, thus leading to negative values for P.

Let us finally comment upon the effect of the pumping fraction n_m^*/n_m on P, shown in figure 8. Very similar types of behaviour are found whatever the line, and we shall discuss here the pumping on the C_9 component, in a case where $\tau_{dep} = \infty$ and $\tau_r = \infty$. At low laser power, i.e. for low P, the results do not depend on n_m^*/n_m ; this is not surprising since in such a case one can make use of a linearized model, such as that developed in [1], in which the relevant parameter for the pumping power is the average pumping time for a ground state atom, namely $\tau_{ij}(N_g/n_m^*)$, which does not depend on n_m^*/n_m (see formula (21)). In con-

trast, at high pumping power, the orientation P increases with the number n_m^* of metastable atoms effectively pumped. This comes from the non-linearities in the orientation coupling between photons and ground state atoms through the n_m^* metastable atoms.

2.4 COMPARISON WITH EXPERIMENTAL RESULTS. — Two parameters n_m^* and τ_{dep} have been put in the model that have to be determined to fit the experimental data. First using the results of optical pumping on the C_9 line, we will be able to assign a value to n_m^* (for this component, τ_{dep} has no effect on the results on the calculation). Fitting the data for another line using the same value of n_m^*, we shall then assign a value to τ_{dep}.

Figure 9 shows the experimental results at 300 K for P when pumping with single frequency laser resonant with the C_9 component (crosses). Circles correspond to the same experiment carried with a laser emitting 3 modes separated by about 150 MHz; furthemore, the beam was reflected back into the cell after a first passage, so that 6 different frequencies within the Doppler profile were absorbed by the atoms. The lines show the results of the calculations for $n_m^*/n_m = 1/120$ (full line), which best fits the single frequency experimental points, and for $n_m^*/n_m = 1/20$ (dashed line), which best fits the experimental data with the 6 frequencies.

Figure 10 is a plot of experimental results obtained at liquid nitrogen temperature ($T = 77$ K), for a single frequency laser (crosses) and the same multimode laser as above (circles). In both cases the central frequency is tuned to the C_9 component. The curves in figure 10 are calculated for $n_m^*/n_m = 1/20$ and for $n_m^*/n_m = 0.3$.

At low laser power, where the results of the calculation do not depend on the adjustable parameter n_m^*, the agreement with the experimental results is satisfactory at both temperatures. In addition, in each of the four experimental situations, a value of n_m^* can be found that allows the model to fit reasonably well with the polarizations measured for the whole accessible range of powers.

Let us remark that the values of the ratio n_m^*/n_m derived from these fits are compatible in all cases with the assumption :

$$\Gamma'/2\,\pi D \ll n_m^*/n_m$$

made in § 1.4.1 for calculating formula (21). (See the values of $\Gamma'/2\,\pi D$ given in appendix B). This means that in all cases the effective number of oriented metastable atoms is larger than the number of atoms directly in resonance with the laser. Comparing results obtained with different laser mode structures, one finds that, both at 300 K and at 77 K, the fraction of atoms effectively oriented (n_m^*/n_m) with a 6-mode laser is of the order of 6 times larger than with a single mode laser.

These results tend to show that the experimental

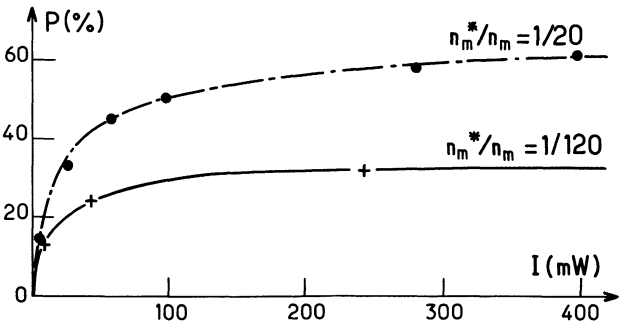

Fig. 9. — Experimental results for the nuclear polarization P as a function of the total laser intensity I at 300 K. The laser is σ^+ polarized, tuned on the C_9 component and covering a surface $S = 18$ cm^2. Crosses refer to a single frequency laser and $T_1 = 95$ s; dots refer to a multimode laser (6 frequencies) and $T_1 = 140$ s. The curves are calculated using $\tau_{dep} = \infty, \tau_r = \infty, p = 0.3$ torr, $n_m/N_g = 2 \times 10^{-6}$, $T_r = T_1$, $n_m^*/n_m = 1/120$ or $n_m^*/n_m = 1/20$.

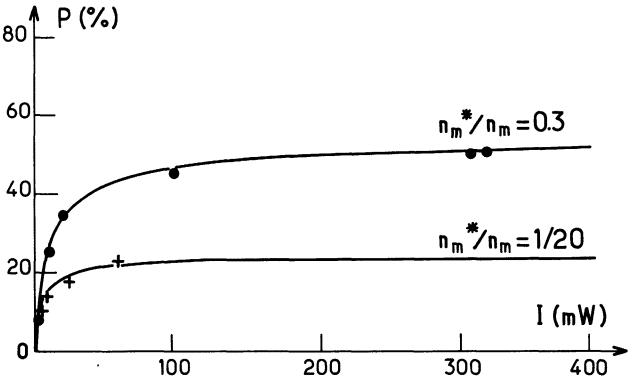

Fig. 10. — Experimental results for the nuclear polarization P as a function of the total laser intensity I at 77 K. The laser is σ^+ polarized on the C_9 component, covering a surface $S = 18$ cm^2. Crosses refer to a single frequency laser, dots refer to a multimode laser (6 frequencies), $T_1 = 108$ s. The curves are calculated using $\tau_{dep} = \infty, \tau_r = \infty, p = 0.3$ torr, $n_m/N_g = 2 \times 10^{-6}$, $T_r = T_1$, $n_m^*/n_m = 1/20$ or $n_m^*/n_m = 0.3$.

results for the nuclear polarization P can be rather well described by a model as crude as that used here, in which the n_m metastable atoms are split into 2 groups (n_m^* interested in the pumping process, $n_m - n_m^*$ only causing relaxation).

In figures 9 and 10 we see that the efficiency of pumping at low laser power does not depend on the mode structure of the laser, as could be expected from the discussion of figure 8. The difference between these efficiencies at 300 K and 77 K comes from the change of Doppler width with temperature (see formula (21) and appendix B) : the absorption of the pumping beam at 77 K is twice that of 300 K, so that the initial slope in figure 10 is the double of that of figure 9. As for the high laser intensity part of these curves one notices that, for any laser configuration, the fraction of metastable atoms effectively oriented

(n_m^*/n_m) is much larger at 77 K than at 300 K. This can be understood from the decrease in efficiency of the metastability exchange collisions when the temperature goes down : each metastable atom has more time at 77 K than at 300 K to undergo velocity changing collisions before making an exchange collision with a ground state atom.

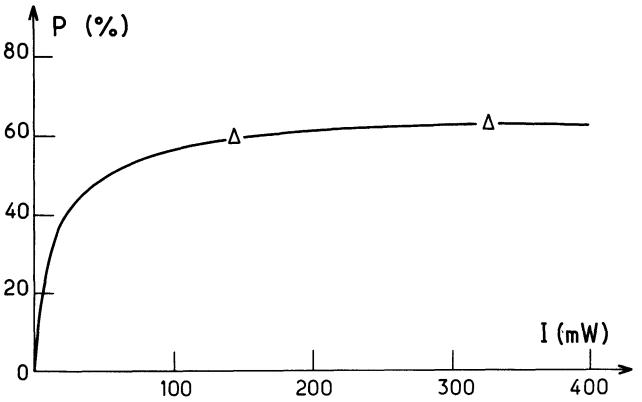

Fig. 11. — Nuclear polarization P as a function of the total laser intensity I at 300 K on $S = 18\ cm^2$. The laser is multimode (6 frequencies) and σ^+ polarized. Its frequency is close to C_5 and adjusted to maximize P. The triangles are experimental. The curve is calculated for $\tau_r = \infty$, $\tau_{dep} = 1.1\ \tau$, $p = 0.3$ torr, $n_m/N_g = 2 \times 10^{-6}$, $T_r = T_1 = 140$ s, $n_m^*/n_m = 1/20$ and a frequency detuning $(\omega - \omega_5^0)/2\pi = 750$ MHz.

Figure 11 shows the results at 300 K obtained when pumping on C_5 with a multimode laser. One must take care that the energy difference between the C_5 transition and the nearby ones is not much larger than the Doppler width ($C_5 - C_4$: 1 480 MHz, $C_5 - C_3$: 1 770 MHz, $C_5 - C_2$: 2 220 MHz), so that one cannot avoid exciting many transitions at the same time, especially at room temperature when $D = 1\ 190$ MHz. The experimental results (triangles) refer to pumping with the laser tuned at a frequency close to that of the C_5 line and adjusted to get as high a nuclear polarization as possible. The curve is calculated with the value $(n_m^*/n_m) = 1/20$ taken from the results obtained when the pumping is on the C_9 component (see Fig. 9), not sensitive to depolarizing collisions in the $2\ ^3P$ state. For figure 11 a best fit is made with τ_{dep} as an adjustable parameter; in addition, to reproduce the experimental conditions the laser frequency is shifted from C_5, in order to maximize the pumping efficiency when adding the contributions of the C_2, C_3, C_4 and C_5 components. An optimum mistuning of 750 MHz is found numerically for a laser intensity of the order of 0.4 W ; it is a compromise between losing polarization when coming too close to C_2, C_3, C_4 components (poorly efficient) and pumping too weakly on C_5. Clearly such a compromise depends on the laser intensity.

The value found in figure 11 for τ_{dep} ($\tau_{dep} = 1.1\ \tau$) shows that collisions in the $2\ ^3P_y$ state do have an effect on the pumping at 0.3 torr, but do not fully equalize the populations of all the sublevels of the $2\ ^3P$ state. Since this collision model is rather crude, the value of τ_{dep} found here should not necessarily well describe the pumping on other C_k components of the line.

2.5 PREDICTIONS OF THE MODEL. — The results of the model given so far are calculated for realistic parameters, corresponding to the present state of the art in optical pumping of ^3He. It is also interesting to discuss the predictions of this model for different experimental conditions that could be met in the future.

Let us first suppose that the laser power becomes very high ([6]). For a laser frequency tuned to the C_8 or C_9 component of the line, the model predicts that, with the same parameters as above (in particular $n_m^*/n_m = 1/20$), P increases up to about 80 % for a laser power of 10 W. The discussion of figure 8 suggests that a larger polarization at high pumping power can be obtained for n_m^*/n_m values closer to 1. Assuming that a different mode structure of the laser allows effective pumping of all the metastable atoms ($n_m^* = n_m$), the model gives that P is of the order of 80 % at 1 W and 90 % at 10 W when pumping on C_8 or C_9 components.

In the discussion of figure 11 we showed that the slightly lower efficiency when pumping on C_5 than pumping on C_8 resulted from the existence of the nearby components. An optimum mistuning of the laser frequency was derived. For much higher laser power, the effect of the C_2, C_3, C_4 components is reduced by using a larger mistuning, so that pumping close to the centre of the C_5 component can give rise to very high nuclear polarizations. For $n_m^*/n_m = 1$, P reaches 92 % at 10 W and 98 % at 100 W with a sufficient mistuning from C_5 (of the order of 3 GHz). For such large frequency mistunings, the absorption of the laser beam is very weak, so that a multi-pass technique with a much weaker beam could lead to the same results.

Another interesting case is when the laser has two different frequencies (in practice it could be achieved with two distinct lasers tuned to different frequencies). For instance, one could think of pumping simultaneously the $F = 1/2$ and $F = 3/2$ hyperfine sublevels of the $2\ ^3S_1$ state, in order to reduce the hyperfine population difference created by the first laser and increase the optical pumping by a sort of « ping-pong effect » between the two hyperfine sublevels, as in sodium [22]. However, for any combination of 2 lasers tuned on 2 different C_k components, the model pre-

([6]) The model is valid even when the transition 2^3S-2^3P is satured by the pumping light beam ; equations (26) and (27) include terms corresponding to stimulated emission.

dicts a value of P lower than that obtained with only one of the 2 frequencies (the more efficient of the 2, pumping with the same intensity as the sum of the intensities of the previous 2 lasers).

3. Conclusion.

This article gives predictions for the best nuclear polarization of helium 3 that one can obtain in a laser optical pumping experiment. Even if it describes the number of metastable atoms effectively pumped and the depolarizing collisions in the 2 ^{3}P state in a rather crude way, the model gives a good understanding of the optical pumping process. It can easily be used for different temperatures, pressures and relaxation rates for instance. The most interesting result is that the model gives correct predictions on how the nuclear polarization depends on the laser characteristics, such as frequency, mode structure and power (including very high power). The maximum value of the nuclear polarization experimentally recorded so far ($P \sim 70\ \%$) is well explained. In order to go beyond this limit, the model suggests that different experimental conditions should be realized. Turning to very large laser power is one possibility, if ever very powerful tunable IR lasers are available. Better compromises could also be eventually found between large metastability exchange rates and low relaxation rates. In this respect a number of proposals are made and discussed in reference [23].

Acknowledgments.

The authors want to thank very much Franck Laloë for his deep interest in this work and for many stimulating discussions and comments on this article.

Appendix A.

The oscillator strength associated to a transition between a two-level atomic system is given by

$$f_{g-e} = \frac{2\,m\omega_0}{\hbar} |\langle e \| R \| g \rangle|^2 \qquad (A.1)$$

where $\langle e \| R \| g \rangle$ is the reduced matrix element of the optical dipole operator, m the electron mass, $\omega_0/2\pi$ the frequency of the atomic transition and $\hbar$ Planck's constant.

In a more general case in which the e and g states both have an angular momentum J_e and J_g one can calculate the oscillator strength $f_{J_g,m_g \to J_e,m_e}$ between a sublevel (J_g, m_g) of the ground state and a sublevel (J_e, m_e) of the excited state. Using the Wigner-Eckart theorem, from (A.1) one obtains :

$$f_{J_g,m_g \to J_e,m_e} = \frac{2\,m\omega_0}{\hbar} \times \frac{1}{2J_e+1} \times \times |\langle J_g, 1, m_g, m_e - m_g | J_e, m_e \rangle|^2 \times |\langle e \| R \| g \rangle|^2 . \qquad (A.2)$$

The total oscillator strength f_{g-e} of the transition can be obtained by summing the partial ones over all excited sublevels, after averaging over the ground state sublevels :

$$f_{g-e} = \frac{1}{(2J_g+1)} \sum_{m_g} \sum_{m_e} f_{J_g,m_g \to J_e,m_e} = \frac{2\,m\omega_0}{\hbar} \times \frac{1}{2J_e+1} \times \frac{1}{2J_g+1} |\langle e \| R \| g \rangle|^2 \qquad (A.3)$$

In the case of the helium 4 transition between the 2 $^3S_1$ and the 2 ^{3}P levels, J_e and J_g refer to $L = 1$ and $L = 0$ respectively. Consequently :

$$f = \frac{2\,m\omega_0}{3\,\hbar} |\langle 2\,^3S_1 \| R \| 2\,^3P \rangle|^2 . \qquad (A.4)$$

The numerical value of f ($f = 0.5391$) can be found in [24]. In the case of the same transition in helium 3, the structure of the transition is more complex, due to hyperfine interaction. However, the total oscillator strength is the same as for helium 4.

In the same way one calculates the inverse of the radiative lifetime τ of any sublevel (J_e, m_e) of the excited state

$$\frac{1}{\tau} = \frac{q^2\,\omega_0^3}{3\,\pi\varepsilon_0\,\hbar c^3} \times \frac{1}{2J_e+1} |\langle 2\,^3S_1 \| R \| 2\,^3P \rangle|^2 \qquad (A.5)$$

from which one derives the relation between $1/\tau$ and f :

$$\frac{1}{\tau} = \frac{2\,\alpha\omega_0^2\,\hbar}{3\,mc^2} f. \qquad (A.6)$$

This leads to

$$\tau = 0.9785 \times 10^{-7}\ \text{s} . \qquad (A.7)$$

Appendix B.

For the $A_i \to B_j$ transition, the absorption probability $1/\tau_{ij}$ is given by equation (10) :

$$1/\tau_{ij} = \gamma_k\, T_{ij}$$

where γ_k is given, according to (17), by

$$\gamma_k = G \frac{(\Gamma'^2/4)}{(\Gamma'^2/4) + (\omega - \omega_k)^2} \qquad G = \frac{4\,\pi\alpha f}{m\omega\Gamma'} \frac{I}{S} \qquad (B.1)$$

α being the fine structure constant :

$$\alpha = \frac{q^2}{4\,\pi\varepsilon_0\,\hbar c} .$$

Formula (B.1) was derived for a laser frequency $(\omega/2\pi)$ and an atomic transition frequency $(\omega_k/2\pi)$, the latter depending upon the velocity v_z of the absorbing metastable atom along the direction of the light beam. If $(\omega_k^0/2\pi)$ is the transition frequency in the frame of the atom, one has :

$$\omega_k = \omega_k^0 \{ 1 + (v_z/c) \} .$$

For a gas at a temperature T, the velocity distribution is :

$$\mathcal{F}(v_z) = \frac{e^{-(v_z/\bar{v})^2}}{\bar{v}\sqrt{2\pi}}$$

where the mean velocity $\bar{v}$ is given by :

$$\bar{v} = \sqrt{\frac{2kT}{m}} .$$

The corresponding transition frequency distribution is thus characterized by the Doppler width D (in frequency units) :

$$D = (\omega_k^0/2\pi)(\bar{v}/c) .$$

For helium 3, the values of $\bar{v}$ and D at the temperatures of interest in this article are :

T (K)	300	77	4.2
$\bar{v}$ (m/s)	1.29×10^3	6.53×10^2	1.52×10^2
D (MHz)	1.19×10^3	6.03×10^2	1.41×10^2

One has now to calculate the average pumping time and hence the average value $\bar{\gamma}_k$ for the ensemble of metastable atoms (with density n_m^*) effectively pumped by the laser. Let us call $\mathcal{F}^*$ the velocity distribution, normalized to 1, of these n_m^* atoms. Assuming that $\mathcal{F}^*$ is centred on the laser frequency $(\omega/2\pi)$, and much broader than the linewidth $(\Gamma'/2\pi)$ of the transition (assumption (20) in the text), $\bar{\gamma}_k$, which is given by :

$$\bar{\gamma}_k = G \cdot \int_{-\infty}^{\infty} \frac{\mathcal{F}^*(v_z)(\Gamma'^2/4)}{(\Gamma'^2/4) + \{ \omega - \omega_k^0 - (\omega_k^0 v_z/c) \}^2} dv_z$$

can be easily derived :

$$\bar{\gamma}_k \simeq G\mathcal{F}^*\left(\bar{v} \cdot \frac{\omega - \omega_k^0}{2\pi D}\right) \times \int_{-\infty}^{\infty} \frac{(\Gamma'^2/4)\, dv_z}{(\Gamma'^2/4) + (\omega_k^0 v_z/c)^2}$$

$$\bar{\gamma}_k \simeq \pi G \frac{c\Gamma'}{2\omega_k^0} \mathcal{F}^*\left(\bar{v} \cdot \frac{\omega - \omega_k^0}{2\pi D}\right).$$

Since all the atoms in resonance with the laser are effectively pumped, their density is the total density for the resonant velocity :

$$n_m^* \mathcal{F}^*\left(\bar{v}\frac{\omega - \omega_k^0}{2\pi D}\right) = n_m \mathcal{F}\left(\bar{v}\frac{\omega - \omega_k^0}{2\pi D}\right) =$$

$$= n_m \frac{\omega_k^0}{(2\pi)^{3/2} cD} e^{-(\omega - \omega_k^0)^2/(2\pi D)^2} .$$

So the expression of $\bar{\gamma}_k$ is finally given by :

$$\bar{\gamma}_k = \sqrt{\frac{\pi}{2}} \frac{I}{S} \frac{\alpha f}{m\omega D} \frac{n_m}{n_m^*} e^{-(\omega - \omega_k^0)^2/(2\pi D)^2} . \quad (B.2)$$

For the conditions of the experiment at 300 K, with a laser frequency tuned on an atomic component, one obtains numerically :

$$\bar{\gamma}_k = 17.5 \times 10^7 \text{ s}^{-1}$$

for $I = 400$ mW on a surface $S = 18$ cm^2.

References

[1] COLEGROVE, F. D., SCHEARER, L. D. and WALTERS, G. K., *Phys. Rev.* **132** (1963) 2561.

[2] COHEN-TANNOUDJI, C. and KASTLER, A., *Progress in Optics,* Vol. V (North Holland Publ. Comp) 1966.

[3] HAPPER, W., *Rev. Mod. Phys.* **44** (1972) 169.

[4] LEFÈVRE-SEGUIN, V., NACHER, P. J., BROSSEL, J., HARDY, W. N. et LALOË, F., *J. Physique* **46** (1985) 1145.
LEFÈVRE-SEGUIN, V., Thèse (Paris, 1984).

[5] LEDUC, M., CRAMPTON, S. B., NACHER, P. J. and LALOË, F., *Nucl. Sci. Appl.* **2** (1984) 1.

[6] Spin polarized quantum systems, *J. Physique Colloq.* **41** (1980) C7 and references therein.

[7] DUPONT-ROC, J., LEDUC, M. et LALOË, F., *J. Physique* **34** (1973) 961 et 977.

[8] TIMSIT, R. S. and DANIELS, J. M., *Canad. J. Phys.* **49** (1971) 545.

[9] NACHER, P. J., LEDUC, M., TRÉNEC, G. et LALOË, F., *J. Physique Lett.* **43** (1982) L-525.

[10] ROSNER, S. D. and PIPKIN, F. M., *Phys. Rev.* **71** (1970) 571.

[11] FRIEZE, W., HINDS, E. A., HUGHES, V. W., PICHANICK, F. M. J., *Phys. Rev.* **A 24** (1981) 279.

[12] KPONOU, A., HUGHES, V. W., JOHNSON, C. E., LEWIS, S. A. and PICHANICK, F. M. J., *Phys. Rev.* **A 24** (1981) 264.

[13] PRESTAGE, J. D., HINDS, E. A. and PICHANICK, F. M. J., *Phys. Rev. Lett.* **50** (1983) 828.

[14] PARTRIDGE, R. B. and SERIES, G. W., *Proc. Phys. Soc.* **88** (1966) 983.

[15] DESCOUBES, J. P., Thesis Paris (1967).

[16] PINARD, M., AMINOFF, C. G. and LALOË, F., *Phys. Rev.* **A 19** (1979) 2366.

[17] AMINOFF, C. G. et PINARD, M., *J. Physique* **43** (1982) 263.

[18] SCHEARER, L. D., Ph. D. thesis, Rice University (1966) ; BYERLY, R., Ph. D. thesis, Rice University (1967).
[19] SCHEARER, L. D. and RISEBERG, L. A., *Phys. Lett.* **33A** (1970) 325.
[20] FITZSIMMONS, W. A., LANE, N. F. and WALTERS, G. K., *Phys. Rev.* **174** (1968) 193 ; BARBÉ, R., Thèse d'Etat, Paris (1977).
[21] NACHER, P. J., LEDUC, M., TRÉNEC, G. et LALOË, F., *J. Physique Lett.* **43** (1982) L-525.
[22] ELBEL, M., HÜHNERMANN, H., MEIER, Th. and SCHNEIDER, W. B., *Z. Phys.* **A 275** (1975) 339.
[23] NACHER, P. J., Thèse d'Etat, Paris (1985).
[24] *Atomic transition probabilities,* W. L. Wiese, M. W. Smith and B. M. Glennon, National Standard Reference Data Series NBS 4 (1966).